

Mesenchymal-like immune-altered is the fourth robust triple-negative breast cancer molecular subtype

Pascal Jézéquel^{1,2,3*}, Hamza Lasla¹, Wilfried Gouraud¹, Agnès Basseville¹, Bertrand Michel⁴, Jean-Sébastien Frenel^{1,2,3}, Philippe P. Juin^{2,3}, Fadoua Ben Azzouz¹, Mario Campone^{1,2,3,5}

¹ Institut de Cancérologie de l'Ouest, F-44805 Saint Herblain, France

² Nantes Université, Univ Angers, INSERM, CNRS, CRCI2NA, F-44000 Nantes, France

³ Équipe Labellisée LIGUE Contre le Cancer CRCI2NA, F-44000 Nantes, France

⁴ Nantes Université, École Centrale Nantes, CNRS, Laboratoire de Mathématiques Jean Leray, LMJL, UMR 6629, F-44000 Nantes, France

⁵ Université d'Angers, F-49000 Angers, France

*Corresponding author Pascal Jézéquel, Omics and Data Science Unit, Institut de Cancérologie de l'Ouest - site René Gauducheau, Bd J. Monod, 44805 Saint Herblain Cedex, France pascal.jezequel@ico.unicancer.fr

Article publié en ligne sur :

<https://doi.org/10.1007/s12282-024-01597-z>

Abstract

Background Robust molecular subtyping of triple-negative breast cancer (TNBC) is a prerequisite for the success of precision medicine. Today, there is a clear consensus on three TNBC molecular subtypes: luminal androgen receptor (LAR), basal-like immune-activated (BLIA) and basal-like immune-suppressed (BLIS). However, the debate about the robustness of other subtypes is still open.

Methods An unprecedented number ($n = 1942$) of TNBC patient data was collected. Microarray- and RNAseq-based cohorts were independently investigated. Unsupervised analyses were conducted using k-means consensus clustering. Clusters of patients were then functionally annotated using different approaches. Prediction of response to chemo- and targeted therapies, immune checkpoint blockade and radiotherapy were also screened for each TNBC subtype.

Results Four TNBC subtypes were identified in the cohort: LAR (19.36%); mesenchymal stem-like (MSL/MES) (17.35%); BLIA (31.06%); and BLIS (32.23%). Regarding the MSL/MES subtype, we suggest renaming it to mesenchymal-like immune-altered (MLIA) to emphasize its specific histological background and nature of immune response. Treatment response prediction results show, among other things, that despite immune activation, immune checkpoint blockade is probably less or completely ineffective in MLIA, possibly caused by mesenchymal background and/or an enrichment in dysfunctional cytotoxic T lymphocytes. TNBC subtyping results were included in the bc-GenExMiner v5.0 webtool (<http://bcgenex.ico.unicancer.fr>).

Conclusions The mesenchymal TNBC subtype is characterized by an exhausted and altered immune response, and resistance to immune checkpoint inhibitors. Consensus for molecular classification of TNBC subtyping and prediction of cancer treatment responses helps usher in the era of precision medicine for TNBC patients.

Keywords:

Triple-negative breast cancer . Subtypes . Mesenchymal-like immune-altered. Treatment prediction . Immune checkpoint blockade

Introduction

Triple-negative breast cancer (TNBC) is a heterogeneous disease which is immunohistochemically characterized by a lack of estrogen receptor (ER), progesterone receptor (PR) and a lack of human epidermal growth factor receptor 2 (HER2) overexpression. It accounts for 12 to 17% of primary BC and is the most aggressive BC subtype [1]. Biological heterogeneity and lack of tumor-specific drug targets and/or alternative therapeutic strategies represent the two main issues for precision treatment of TNBC patients. Improved subtype classification and identification of therapeutic pathways are therefore urgently needed to optimize patient care. In particular, immunotherapy and, more precisely, the use of immune checkpoint blockade (ICB), represents an important breakthrough in the treatment of TNBC [2]. However, one key problem for ICB resides in the identification of specific biomarkers for prediction of response to immune checkpoint (IC) inhibitors since PD-L1 expression, measured by immunohistochemistry (IHC), was reported as an imperfect ICB biomarker [3, 4]. Computational immuno-transcriptomics is a solution to address this problem [5].

Several studies have developed specific molecular classifications for TNBC based on gene expression profiles [6-10]. To date, three to six numbers of transcriptome-based TNBC subtypes have been identified (Table S1). The differences in the numbers of TNBC subtypes arise for various reasons (Table S1) [11]. Additional omics approaches have also been used to subtype TNBC [12-16].

Today, there is a clear consensus on three TNBC robust subtypes: luminal androgen receptor (LAR); basal-like immune-activated (BLIA); basal-like immune-suppressed (BLIS). There is open debate about the nature and robustness of other subtypes, notably mesenchymal-like (M), which is characterized by mesenchymal differentiation, high proliferation and cell motility, and mesenchymal stem-like (MSL or MES), which is characterized by mesenchymal features, stem-cell features, low proliferation and claudin-low gene expression, and high angiogenesis-related gene expression [17]. In 2016, Lehmann and colleagues revised their initial classifications, reducing them from six subtypes to four [18]. Immunomodulatory (IM) and MSL/MES subtypes were eliminated because of a high level of tumor-infiltrating immune and stromal cells, respectively. In the following years, two transcriptomic studies managed to identify M and MSL/MES, while three others failed to do so [11, 19-22]. Another important question concerns the type and level of immune response in these two mesenchymal subtypes compared to IM/BLIA, notably immune checkpoint expressions, because ICB is at stake [23-26]. Immune response is low in M with no observable expression of immune checkpoint [17, 18, 27, 28]. On the contrary, MSL/MES is characterized by a high immune response and expression of immune checkpoints, as is the case for BLIA [16, 17, 28, 29]. Furthermore, despite not being identified in Rody's study, MSL/MES subtype with a high immune response is present [30]. Thus, high immune response is a true biological characteristic of MSL/MES.

Here, our goal was to establish a consensus for molecular classification of TNBC. Then, we sought to predict responses to chemo- and targeted therapies, ICB and radiotherapy in each of these subtypes. To optimize this process, we harvested the largest possible amount of transcriptomic data from public repositories, measured by microarray and RNAseq. To our knowledge, this is the largest study aimed at subtyping TNBC; it exploits a total of 1942 samples.

We concluded that TNBC are composed of four robust subtypes: LAR, BLIA, BLIS and MES. More importantly, we propose that this last subtype should be renamed to mesenchymal-like immune-altered (MLIA), as this term highlights its two main biological characteristics, i.e., mesenchymal-like features and an altered immune response. Despite immune activation, comparable to that of BLIA, ICB is probably less or not at all effective in MLIA, possibly caused by mesenchymal background and/or an enrichment in dysfunctional cytotoxic T lymphocytes (CTL).

As an extension of this work, these results (TNBC cohorts and TNBC subtypes) were included in the bc-GenExMiner database (<http://bcgenex.ico.unicancer.fr>) [31-33].

Materials and Methods

TNBC clinicopathological and transcriptomic data

The selection of transcriptomic datasets was done according to the following inclusion criteria: tumor cells negative for ER, PR and without HER2 overexpression; female BC; invasive carcinomas; metastasis-free at diagnosis; fresh-frozen tumor; no neoadjuvant therapy before tumor collection; minimum number of patients per cohort n = 28. We looked for publicly available TNBC transcriptomic data sets in repositories and in articles complying with our inclusion criteria. All microarrays and RNAseq data met acceptable quality levels. Available clinicopathological data linked to these data were also harvested.

Gene expression data pre-processing

AffymetrixTM microarrays raw data were MAS5 normalized using AffymetrixTM expression console software version 1.3.1 using default settings, and then log2-transformed. Agilent microarrays raw data were loess normalized then log2 transformed sample/reference intensity ratios. When multiple probes were mapped to the same gene, the median value was calculated as the expression value of this gene. RNAseq data were acquired in raw counts or already in fragments per kilobase of transcript per million (FPKM). FPKM values were then log2-transformed with an offset of 0.1 to avoid undefined values. Genes with zero variance were excluded. For each cohort (microarray or RNAseq): 1) only genes shared across all studies were kept and 2) all datasets were merged into one by using the empirical Bayes algorithm (ComBat function) to remove batch effect.

Unsupervised analysis

Unsupervised k-means consensus clustering was performed to identify TNBC subtypes. The following parameters were used: 10 maximum clusters; 1000 iterations; and 0.8 subsampling fraction. Identification of the optimal number of genes was accomplished by selecting the most variable genes from 500 to 5000 in increments of 500, and evaluating the best clustering result using silhouette criterion. Finally, the optimal number of clusters was determined using the cumulative distribution function.

Cluster functional annotation

Clusters were annotated with: 1) clinicopathological characteristics; 2) gene ontology enrichment analyses (GOEA) based on biological process terms of 2-1) the 50 most contributing genes to the construction of the two principal components (PC1 and PC2), 2-2) differential gene expressions (DGE) between clusters and 2-3) discriminant clusters of highly expressed genes; 3) gene set enrichment analysis (GSEA) (see next section); 4) 73 gene expression signatures (GES) for biological pathway exploration; 5) 47 IC mRNA expression (Table S2).

Pathway enrichment analysis was performed using fgsea package with all genes ranked by T-test and the gene ontology biological process pathway database (R msigdbr package). Enriched pathways were then filtered by selecting the ones with a normalized enrichment score > 0 combined with an adjusted P < 0.001. Redundancy in filtered pathways was identified by semantic similarity (Wang distance method) using R rrvgo package, and the pathway number was reduced accordingly to reach a maximum of 20 pathways by increasing the similarity threshold (from 0.7 to 0.95 in increments of 0.1).

Treatment prediction

Prediction model and GES approaches were used to predict response to different cancer therapies: chemo- and targeted therapies, using R OncoPredict and its original version (R pRRophetic) packages (198 drugs screened) [34]; ICB using TIDE algorithm; radiotherapy, using four GES (Table S2).

Statistical analysis

Quantitative variables were summarized using mean and standard deviation and were compared using Student's t-test or one-way analysis of variance (ANOVA) with a Tukey post hoc test, as appropriate. Categorical variables were summarized using count and percentage and were compared using chi-square or Fisher's exact test, as appropriate. Survival probability was estimated using the Kaplan–Meier method and compared between subtypes by Log-rank test. DGE analyses were performed using the R/Bioconductor limma package. Genes with $|\log_{2}FC| \geq 1.5$ and adjusted $P < 0.01$ were considered significant. Highly expressed genes were represented on a heatmap, with patients ordered according to subtype. Hierarchical clustering was performed for genes and patients. Pearson's correlation coefficient was used to calculate the correlation. GES scores, IC mRNA expressions and correlation matrix between GES were represented as heatmaps using hierarchical clustering with centered Pearson's correlation and average linkage methods. The Benjamini-Hochberg procedure was employed to correct for multiple testing. We considered a two-sided P of less than 0.05 to be statistically significant.

bc-GenExMiner

TNBC subtyping results were included in the bc-GenExMiner database. More details about its design, construction and coding can be found in previous articles [31-33].

Results

TNBC transcriptomic and clinicopathological data

A total of 1942 TNBC patient's data were collected from 19 datasets, with 1243 samples from microarray technology (14 datasets including two internal cohorts, already published) and 699 from RNAseq technology (five datasets including one new internal cohort) (Table S3). Due to the merging of datasets issued from different platforms for both technologies, only common genes were kept with 14,514 genes for the microarray cohort and 15,614 for the RNAseq cohort. Clinicopathological data were also gathered when available (Table S3). Microarray- and RNAseq-based cohorts were investigated independently throughout the study.

Unsupervised analysis confirmed four molecular subtypes

Consensus k-means clustering separated TNBC microarray and RNAseq TNBC cohorts into four optimal clusters using the 2000th and 1500th most variable genes, respectively. After their biological characterization, clusters were named as follows (detailed in the next section): LAR, MLIA, BLIA and BLIS. Distributions of patients among the four clusters in the two cohorts were similar ($P = 0.2303$). Distributions were also similar between studies for the microarray cohort ($P = 0.2479$) and RNAseq cohort ($P = 0.1775$). Pooled data ($n = 1942$ patients) had the following distribution: 19.36% for LAR; 17.35% for MLIA; 31.06% for BLIA; 32.23% for BLIS, confirming that TNBC are largely, but not exclusively, basal-like (63.29%).

Cluster functional annotation

Clinicopathological characteristics

Some significant clinicopathological differences exist between the four subtypes in both cohorts (Table 1). LAR patients are significantly older, have low-grade tumors, Nottingham prognostic index and Ki67. Furthermore, follow-up analyses show survival differences between the four subtypes: disease-free survival (DFS), $P = 0.0019$; distant metastasis-free survival (DMFS), $P = 0.0136$ (Fig. 1). MLIA and BLIS are associated with the best and the worst prognoses, respectively. In the RNAseq cohort, no survival differences were observed between the four subtypes: DFS, $P = 0.7535$; DMFS, $P = 0.6232$; overall survival (OS), $P = 0.2804$.

The following biological characterization was performed by only keeping common results between the two cohorts to increase the robustness of the findings.

a.

Variable	All n = 1243 (%)	LAR n = 239 (%)	MLIA n = 216 (%)	BLIA n = 404 (%)	BLIS n = 384 (%)	p
Age (years; mean ± sd)	53.9 ± 12.6	59.5 ± 12.3	52.1 ± 12.1	51.3 ± 11.5	54.2 ± 13.0	< 0.0001
Nodal status	Negative 460 (51.1) Positive 440 (48.9)	87 (45.3) 105 (54.7)	67 (46.2) 78 (53.8)	146 (50.3) 144 (49.7)	160 (58.6) 113 (41.4)	0.0170
Tumour size (mm; mean ± sd)	26.0 ± 14.7	26.8 ± 14.9	21.8 ± 11.6	26.4 ± 16.9	27.1 ± 13.1	0.0367
Histological types	IDC 853 (96.5) ILC 31 (3.5)	167 (89.8) 19 (10.2)	143 (96.6) 5 (3.4)	273 (99.3) 2 (0.7)	270 (98.2) 5 (1.8)	< 0.0001
SBR grade	1 15 (1.5) 2 161 (17.0) 3 773 (81.5)	7 (3.7) 65 (34.2) 118 (62.1)	3 (1.9) 35 (22.2) 120 (75.9)	2 (0.6) 21 (6.8) 287 (92.6)	3 (1.0) 40 (13.8) 248 (85.2)	< 0.0001
NPI	1 31 (4.8) 2 416 (64.2) 3 201 (31.0)	16 (12.7) 70 (55.6) 40 (31.7)	5 (4.9) 66 (64.7) 31 (30.4)	5 (2.4) 137 (64.3) 71 (33.3)	5 (2.4) 143 (69.1) 59 (28.5)	0.0020
Ki67	< 20 54 (19.0) ≥ 20 230 (81.0)	23 (40.4) 34 (30.4)	10 (21.7) 15 (41.7)	5 (5.4) 8 (8.2)	16 (18.0) 15 (17.2)	< 0.0001
P53 status (IHC)	No 42 (36.8) Yes 72 (63.2)	18 (64.3) 10 (35.7)	6 (31.6) 13 (68.4)	12 (30.0) 28 (70.0)	6 (22.2) 21 (77.8)	0.0057
TP53 status (seq)	No 56 (20.3) Yes 220 (79.7)	18 (32.1) 38 (67.9)	15 (41.7) 21 (58.3)	8 (8.2) 89 (91.8)	15 (17.2) 72 (82.8)	< 0.0001
TILs	≤ 20 69 (80.2) > 20 17 (19.8)	15 (88.2) 2 (11.8)	7 (53.8) 6 (46.2)	16 (64.0) 9 (36.0)	31 (100.0) 0 (0.0)	0.0001
BRCA1	No 296 (89.7) Yes 34 (10.3)	58 (96.7) 2 (3.3)	42 (87.5) 6 (12.5)	102 (87.9) 14 (12.1)	94 (88.7) 12 (11.3)	0.2207
BRCA2	No 320 (97.3) Yes 9 (2.7)	57 (95.0) 3 (5.0)	46 (97.9) 1 (2.1)	114 (98.3) 2 (1.7)	103 (97.2) 3 (2.8)	0.6209
BRCA1/2	No 287 (87.0) Yes 43 (13.0)	55 (91.7) 5 (8.3)	41 (85.4) 7 (14.6)	100 (86.2) 16 (13.8)	91 (85.8) 15 (14.2)	0.6945
Chemotherapy	No 133 (24.7) Yes 406 (75.3)	32 (30.2) 74 (69.8)	20 (25.6) 58 (74.4)	35 (19.1) 148 (80.9)	46 (26.7) 126 (73.3)	0.1576
Hormone therapy	No 459 (85.5) Yes 78 (14.5)	91 (85.8) 15 (14.2)	65 (82.3) 14 (17.7)	151 (83.4) 30 (16.6)	152 (88.9) 19 (11.1)	0.4105
Radiotherapy	No 87 (17.0) Yes 424 (83.0)	19 (18.6) 83 (81.4)	14 (19.2) 59 (80.8)	26 (15.2) 145 (84.8)	28 (17.0) 137 (83.0)	0.8431
Metastasis	No 603 (71.3) Yes 243 (28.7)	118 (69.8) 51 (30.2)	110 (79.7) 28 (20.3)	201 (73.4) 73 (26.6)	174 (65.7) 91 (34.3)	0.0220
Race	Asian 198 (25.0) Caucasian 593 (75.0)	44 (27.0) 119 (73.0)	34 (23.6) 110 (76.4)	56 (23.0) 187 (77.0)	64 (26.6) 177 (73.4)	0.7295

b.

Variable	All n = 699 (%)	LAR n = 137 (%)	MLIA n = 121 (%)	BLIA n = 199 (%)	BLIS n = 242 (%)	p
Age (years; mean ± sd)	55.8 ± 13.5	63.5 ± 11.3	54.3 ± 11.7	53.2 ± 13.7	54.3 ± 13.8	< 0.0001
Nodal status	Negative 385 (61.6) Positive 240 (38.4)	55 (44.0) 70 (56.0)	63 (58.9) 44 (41.1)	107 (60.8) 69 (39.2)	160 (73.7) 57 (26.3)	< 0.0001
Tumor size (mm; mean ± sd)	25.4 ± 12.9	26.9 ± 14.9	23.0 ± 9.6	28.5 ± 15.3	23.3 ± 10.1	0.0005
Histological types	IDC 449 (98.0) ILC 9 (2.0)	95 (95.0) 5 (5.0)	84 (98.8) 1 (1.2)	122 (99.2) 1 (0.8)	148 (98.7) 2 (1.3)	0.1510
SBR grade	1 4 (0.7) 2 98 (17.9) 3 445 (81.4)	1 (0.9) 47 (44.4) 58 (54.7)	1 (1.1) 24 (24.7) 72 (74.2)	0 (0.0) 4 (2.7) 145 (97.3)	2 (1.0) 23 (11.8) 170 (87.2)	< 0.0001
NPI	1 33 (6.9) 2 290 (60.7) 3 155 (32.4)	14 (14.6) 50 (52.1) 32 (33.3)	6 (7.2) 53 (63.9) 24 (28.9)	2 (1.6) 69 (54.3) 56 (44.1)	11 (6.4) 118 (68.6) 43 (25)	0.0002
Ki67	< 20 51 (9.2) ≥ 20 505 (90.8)	29 (26.1) 82 (73.9)	7 (6.9) 95 (93.1)	7 (4.6) 146 (95.4)	8 (4.2) 182 (95.8)	< 0.0001
TP53 status (seq)	No 22 (25.6) Yes 64 (74.4)	2 (20.0) 8 (80.0)	7 (43.8) 9 (56.2)	5 (16.1) 26 (83.9)	8 (27.6) 21 (72.4)	0.2365
TILs	≤ 20 68 (65.4) > 20 36 (34.6)	12 (70.6) 5 (29.4)	8 (61.5) 5 (38.5)	21 (55.3) 17 (44.7)	27 (75.0) 9 (25.0)	0.3165
BRCA1	No 277 (89.6) Yes 32 (10.4)	55 (100.0) 0 (0.0)	45 (88.2) 6 (11.8)	81 (86.2) 13 (13.8)	96 (88.1) 13 (11.9)	0.0465
BRCA2	No 298 (96.8) Yes 10 (3.2)	54 (98.2) 1 (1.8)	51 (100.0) 0 (0.0)	91 (98.9) 1 (1.1)	102 (92.7) 8 (7.3)	0.0436
BRCA1/2	No 269 (86.8) Yes 41 (13.2)	54 (98.2) 1 (1.8)	45 (88.2) 6 (11.8)	80 (85.1) 14 (14.9)	90 (81.8) 20 (18.2)	0.0305
Chemotherapy	No 77 (12.5) Yes 538 (87.5)	21 (16.9) 103 (83.1)	8 (7.5) 98 (92.5)	18 (10.5) 154 (89.5)	30 (14.1) 183 (85.9)	0.1250
Hormone therapy	No 265 (96.7) Yes 9 (3.3)	38 (92.7) 3 (7.3)	40 (95.2) 2 (4.8)	85 (95.5) 4 (4.5)	102 (100.0) 0 (0.0)	0.0324
Radiotherapy	No 298 (62.2) Yes 181 (37.8)	65 (62.5) 39 (37.5)	58 (67.4) 28 (32.6)	63 (48.1) 68 (51.9)	112 (70.9) 46 (29.1)	0.0007
Metastasis	No 129 (95.6) Yes 6 (4.4)	18 (90.0) 2 (10.0)	20 (95.2) 1 (4.8)	46 (95.8) 2 (4.2)	45 (97.8) 1 (2.2)	0.5044
Race	Asian 366 (52.5) Caucasian 307 (44.0) Others 24 (3.5)	89 (65.0) 48 (35.0) 0 (0.0)	68 (56.2) 48 (39.7) 5 (4.1)	90 (45.7) 96 (48.7) 11 (5.6)	119 (49.2) 115 (47.5) 8 (3.3)	0.0019

Table 1. Clinicopathological characteristics of TNBC in function of cluster assignment. a microarray cohort. b RNAseq cohort (IDC: invasive ductal carcinoma; IHC: immunohistochemistry; ILC: invasive lobular carcinoma; NPI: Nottingham prognostic index; seq: sequence-based; TILs: tumor infiltrating lymphocytes)

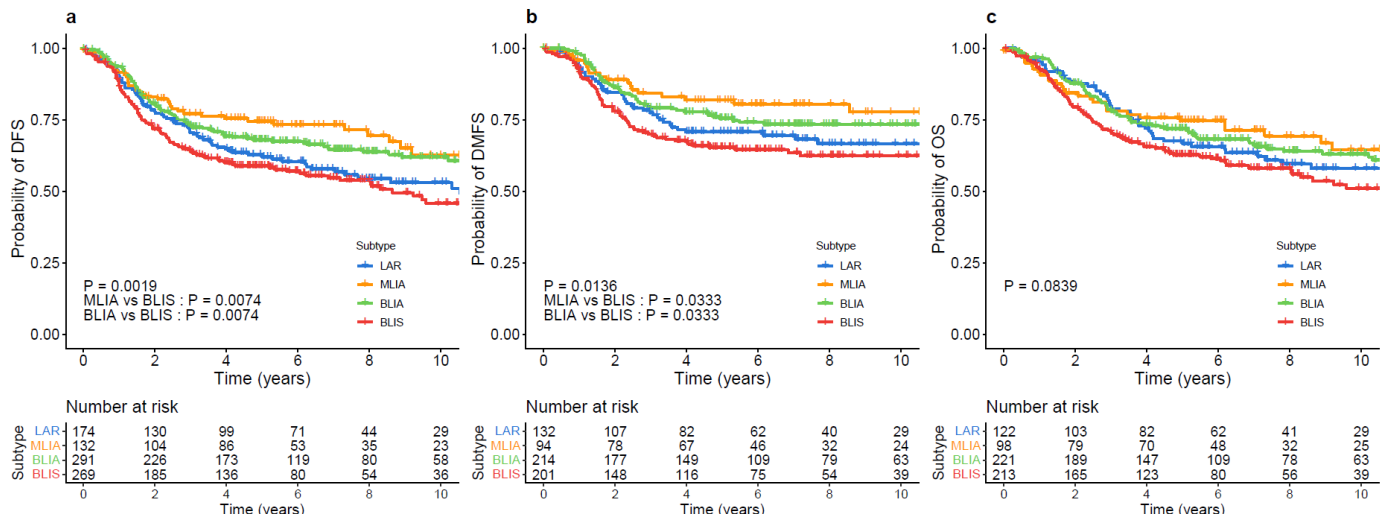


Figure 1. Kaplan-Meier survival curves for microarray TNBC cohort. a DFS. b DMFS. c OS.

Pathway enrichment analysis

We performed principal component analysis (PCA) on the two cohorts to identify genes explaining variation across subtypes. PCA separates the four clusters according to three biological characteristics: androgen receptor pathway (ARP), which is inversely correlated to migration and invasion, for PC1, and immune response, for PC2 (Fig. 2; Table S4).

To improve the completeness and robustness of pathway annotation, two pathway enrichment analysis methods (overrepresentation-based [LIMMA and heatmap of highly expressed gene results as inputs] and ranking-based methods [GSEA]) were used to characterize molecular pathways associated with each subtype. In summary, LAR is characterized by ARP activation, lipid metabolic process, organic acid metabolic process and response to xenobiotic stimulus; MLIA is characterized by immune response, ARP activation, lipid metabolic process, angiogenesis and claudin-low; BLIA is characterized by immune response and mitotic cell cycle, and BLIS is characterized by mitotic cell cycle, extracellular matrix organization, intermediate filament organization, epithelium development, tissue morphogenesis and neurogenesis (Fig. 3; Table S5).

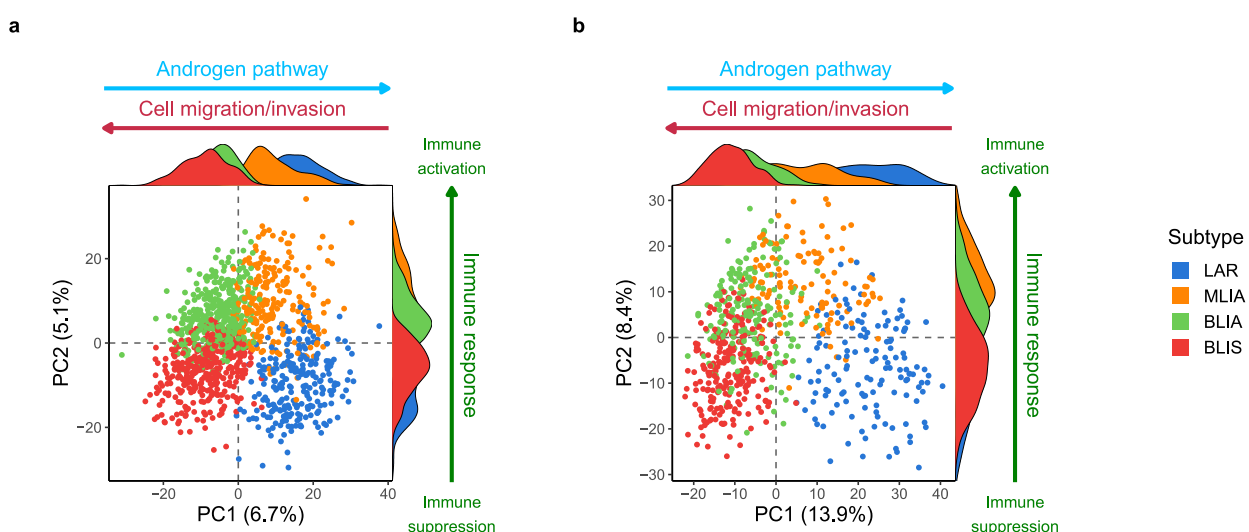


Figure 2. Principal component analyses. Projection of the patients on the first plan. a TNBC microarray cohort (n = 1243). b TNBC RNAseq cohort (n = 699). Associated pathways were defined by enrichment analyses using ToppGene suite with enrichment gene sets composed of the top-50 contributing genes from first (PC1) and second (PC2) principal components

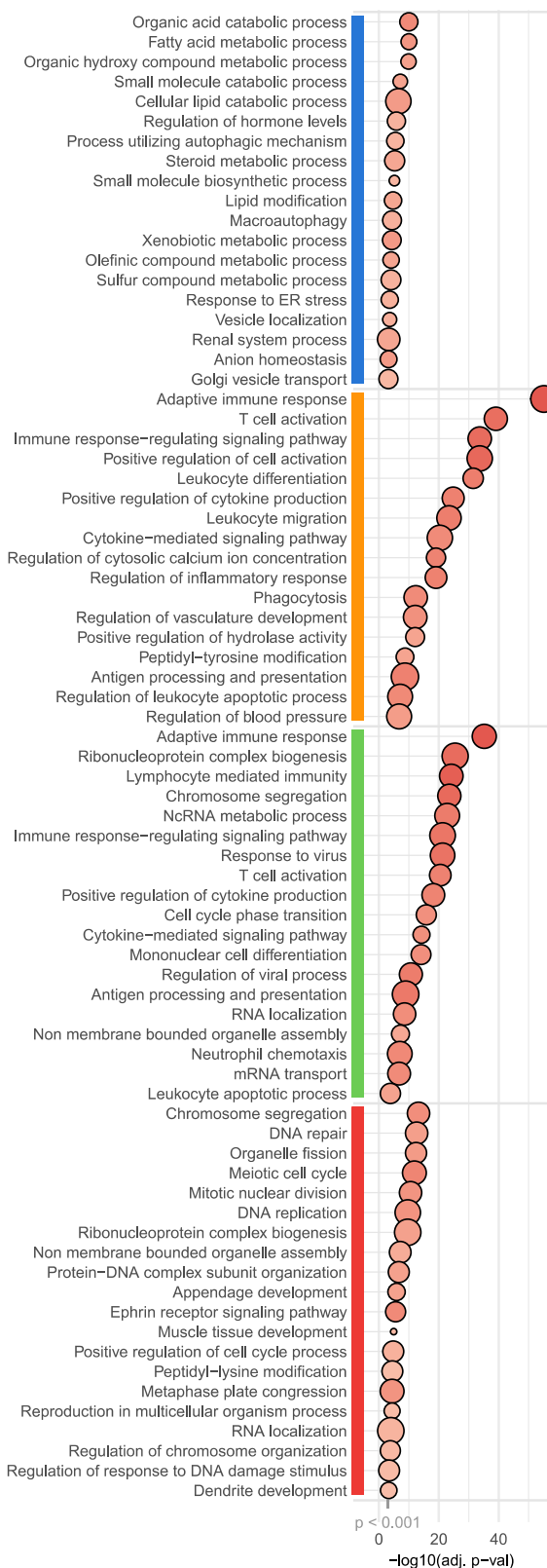
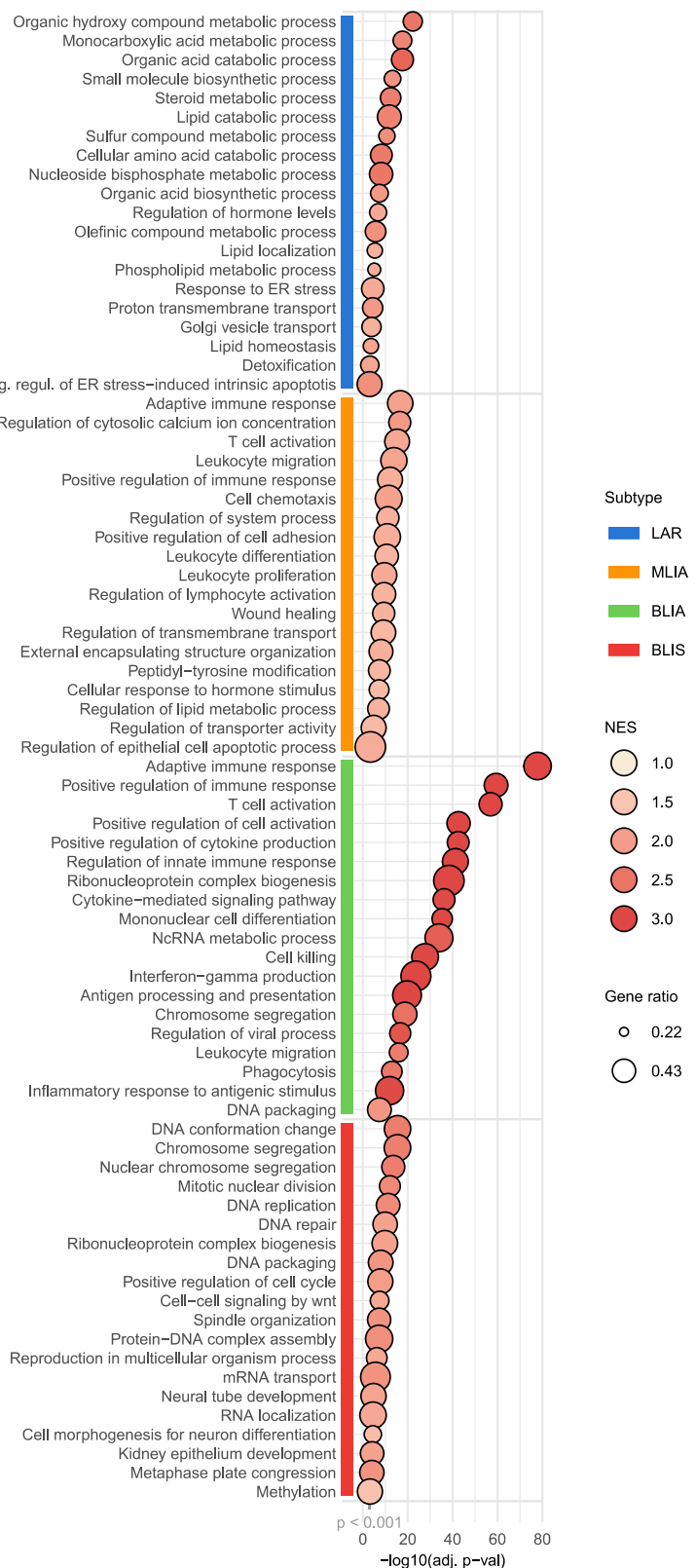
a.**b.**

Figure 3. Gene set enrichment analysis (GSEA). GSEA analysis was performed on t-test ranked genes using fgsea package. Resulting pathways were first filtered by selecting pathways with normalized enrichment scores (NES) > 0 and $P < 0.001$, then a second filtration using semantic similarity was performed to decrease redundancy in pathways and reach 20 pathways maximum for each subtype. **a** TNBC microarray cohort ($n = 1243$). **b** TNBC RNAseq cohort ($n = 699$).

Gene expression signature scores and immune checkpoint mRNA expressions for the four TNBC subtypes

To explore the two cohorts by integrating prior knowledge on BC, we characterized them further using 73 GES as well as 47 immune checkpoint mRNAs. Six clusters of correlation based on GES scoring for microarray and RNAseq TNBC cohorts highlight important biological features of TNBC: basal-like, claudin-low, immune-suppression, immune-activation, mesenchymal stem-like and luminal, which are more or less pronounced in each subtype (Figure S2).

Subsequently, we will only discuss the results obtained for MLIA functional annotation. The results obtained for the other subtypes are presented in Fig. 4, Fig. 5, Table S6 and Table S7.

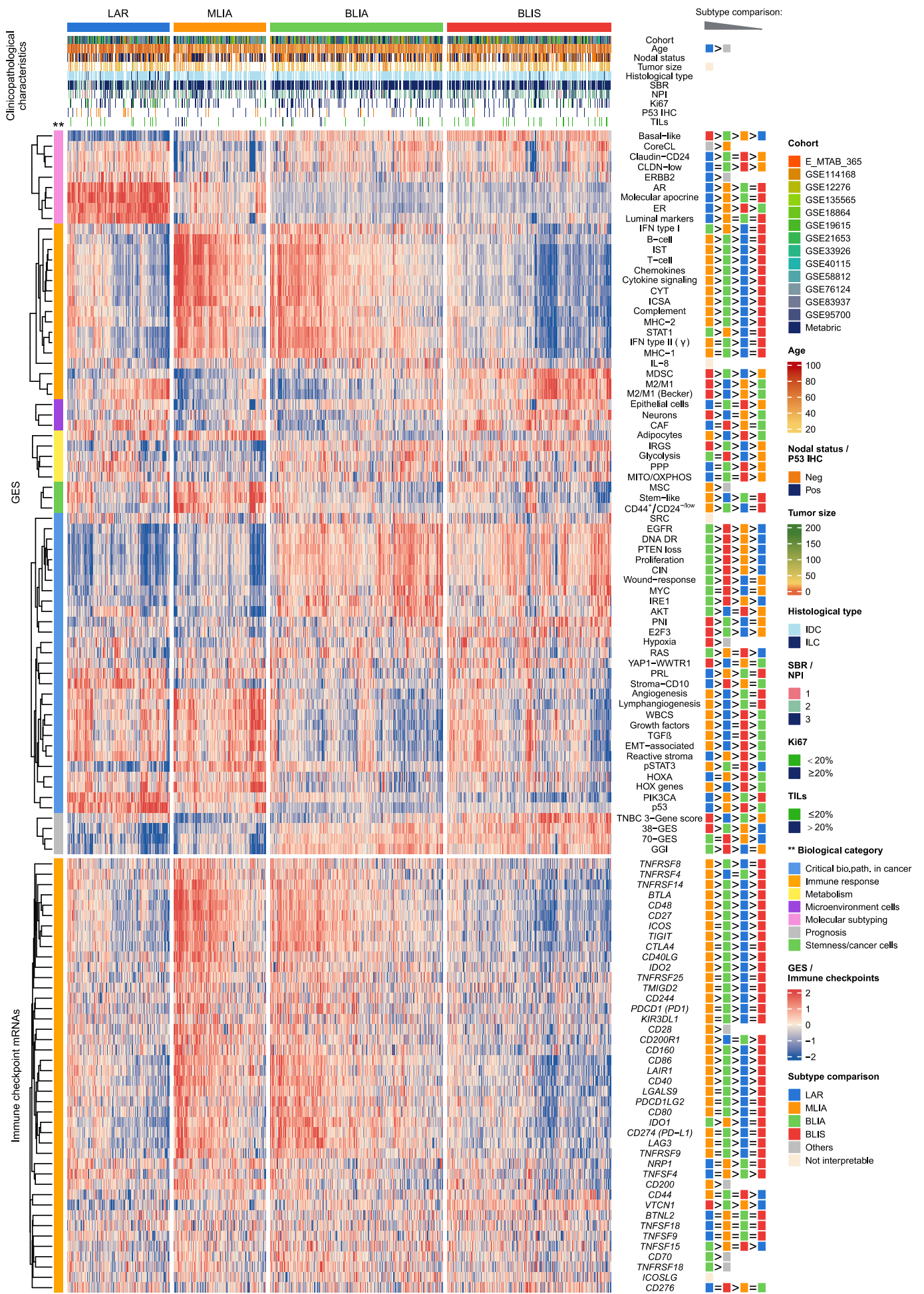
Mesenchymal-like immune-altered

The lowest scores for the three claudin-low GES are observed among MLIA, suggesting that this subtype is enriched in claudin-low tumors (Fig. 4; Fig. 5; Table S6). Fourteen immune response GES scores and 26 out of 41 immune checkpoint mRNA expressions, including CD274 (PD-L1) and PDCD1 (PD1), show that MLIA immune response is higher compared to the two non-immune-activated subtypes, i.e., LAR and BLIS. Six, sixteen and four immune checkpoints display “MLIA > BLIA”, “BLIA > MLIA” and “MLIA = BLIA” profiles, respectively. At first, these results highlight immune activation and the presence of exhausted T cells in this subtype comparable to that of BLIA. Indeed, co-expression of multiple immune inhibitory receptors is considered a cardinal feature of T cell exhaustion [35, 36]. However, and importantly, a crucial difference is pointed out between the two immune-activated subtypes, i.e., MLIA and BLIA. CTL dysfunction GES scores are higher in MLIA than in BLIA, meaning that MLIA is enriched in dysfunctional CTL compared to BLIA. For this very reason, we have chosen the term "altered" to describe the immune response of this subtype.

Four out of the five metabolism GES: glycolysis, iron regulatory gene signature, MITO/OXPHOS and pentose phosphate pathway, show the lowest scores for MLIA, which means that this subtype is less aggressive than the others [37-39]. In addition, MLIA displayed the highest scores for adipocyte GES, which is consistent with Burstein's results [29].

CD44+/CD24-/low, mesenchymal stem cell and stem-like GES scores are high for MLIA. Indeed, CD44+/CD24-/low cells are considered as tumor-initiating cells and are encountered in claudin-low and mesenchymal tumors, here MLIA [40-43]. Reinforcing this result, ALDH1A1 mRNA, which is a marker of stem cells and tumor initiating cells, is highly expressed in MLIA compared to the other subtypes (Figure S3) [44]. Eight critical biological pathways in cancer GES display the highest scores for MLIA compared to the other subtypes: angiogenesis, epithelial-mesenchymal transition (EMT)-associated, growth factors, Hox genes, lymphangiogenesis, pSTAT3, TGF β and Wnt/ β -catenin signaling. Furthermore, proliferation GES scores are lower in this subtype compared to the two basal-like subtypes. The majority of these results demonstrate the mesenchymal and stemness nature of this low-proliferative subtype [17, 28, 36, 40, 45-47]. Moreover, MLIA is characterized by low AKT and MYC GES scores. Hence, targeted inhibitors should not be prescribed for this subtype. And finally, prognostic GES scores in MLIA are low compared to basal-like subtypes. Note that some commonalities exist between MLIA and LAR (e.g., ARP activation), and MLIA and BLIA (e.g., immune activation, including high T-cells and IC mRNA levels) Fig. 5.

In conclusion, MLIA is mainly characterized by EMT, stemness, altered immune response and claudin-low features [43, 48]. Survival analyses show that this subtype is less aggressive compared to the other three (Fig. 1). Concerning MLIA, it is important to underline that immune response, comparable to that of BLIA, is insufficiently highlighted in the literature [22, 29, 40]. The main difference between the two immune-activated subtypes is the enrichment of dysfunctional CTL in MLIA compared to BLIA.

a.

b.

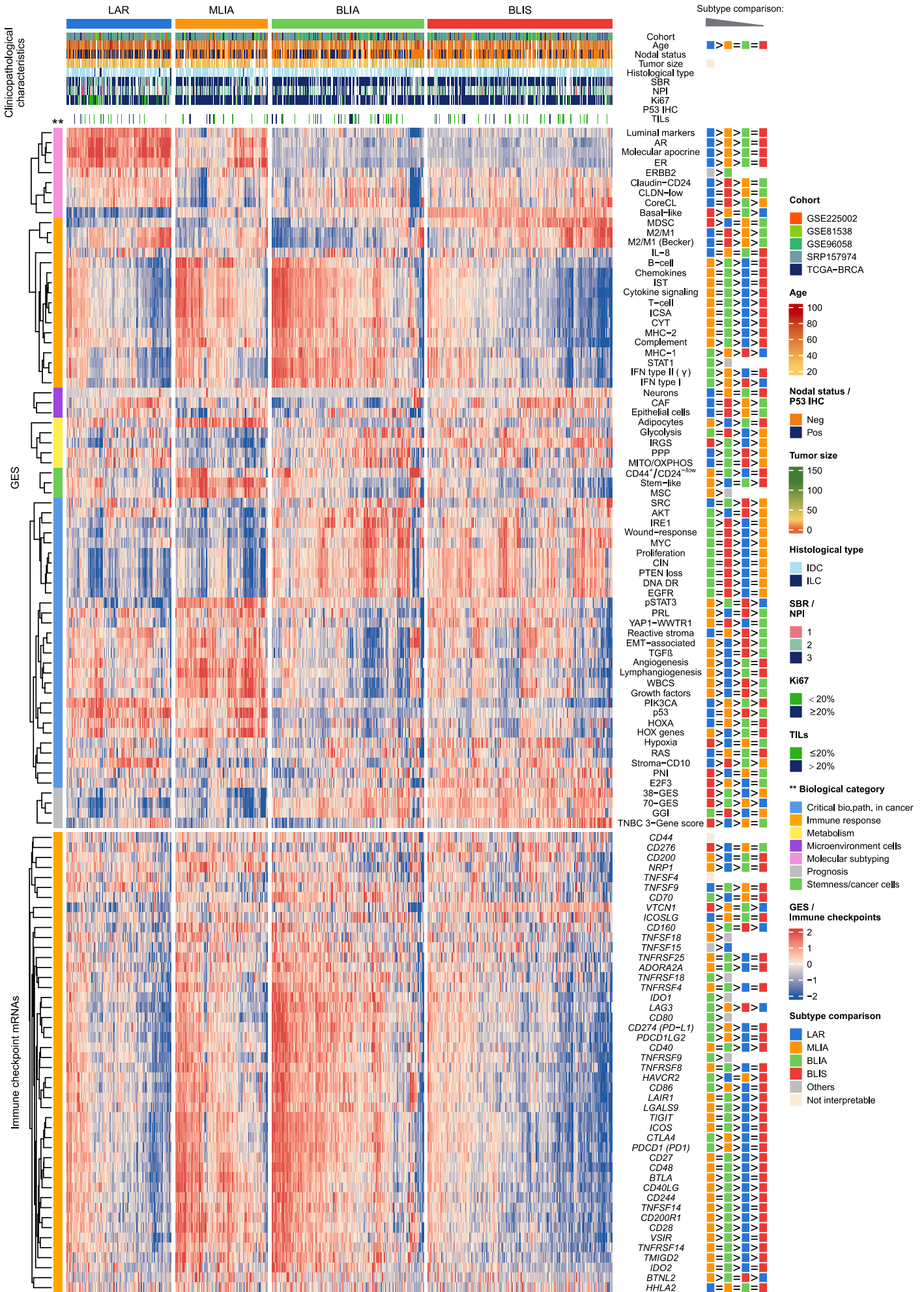


Figure 4 (2 previous pages): Cluster functional annotation. Patients and their clinicopathological characteristics were hierarchically clustered within each subtype according to GES scores combined with immune checkpoint gene expressions. GES variables were clustered within each biological category (left row annotation). For continuous variables, subtype pairwise comparison was performed based on subtype mean value (Tukey post hoc test) and results were summarized and annotated on the heatmap accordingly. a TNBC microarray cohort ($n = 1243$). b TNBC RNAseq cohort ($n = 699$).

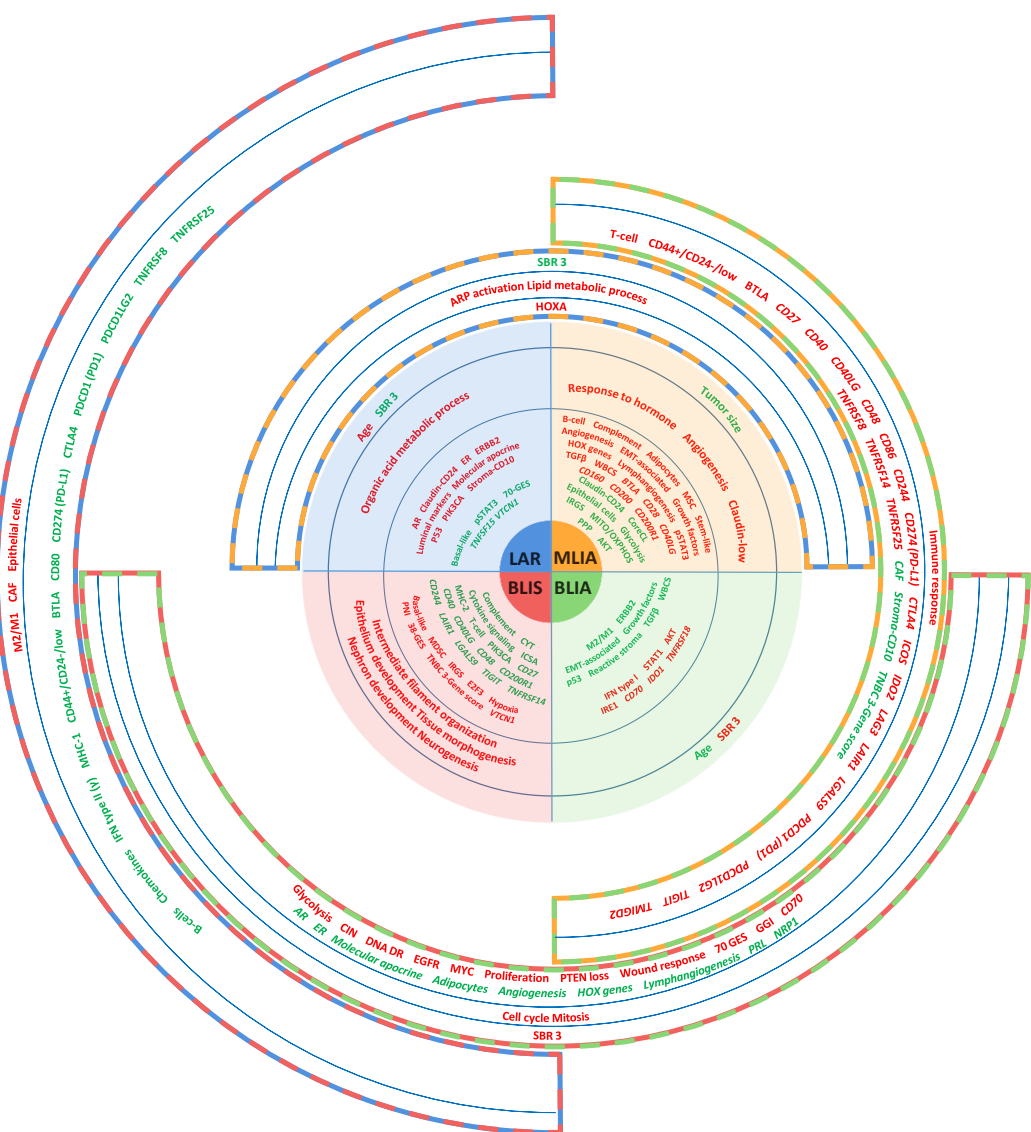


Figure 5. Overview of the clinicopathological and biological characteristics of the four TNBC subtypes. The inner pie chart represents specific results for LAR, MLIA, BLIA and BLIS, and the outer circular segments represent commonalities between two subtypes: LAR and MLIA (blue and orange dashed border); MLIA and BLIA (orange and green dashed border); BLIA and BLIS (green and red dashed border); BLIS and LAR (red and blue dashed border). In each circular segments, from outside to inside, clinicopathological characteristics, pathway enrichment analyses, and GES scores and IC mRNA levels results are shown (green: low; red: high). Only common results between microarray and RNAseq cohorts have been reported.

Treatment prediction

To estimate the difference in drug sensitivity among TNBC subtypes, an in silico pharmacological screening was performed using Oncopredict and pRRophetic packages, which predict the half-maximal concentration (IC_{50}) for ~200 pharmacological inhibitors from the Genomics of Drug Sensitivity in Cancer database, based on transcriptomic data. Chemo- and targeted therapy resistance and sensitivity for each subtype were defined by an IC_{50} strictly superior or inferior to the three other subtypes, respectively, with concordant results between microarray and RNAseq data (Fig. 6).

MLIA seems to be sensitive to drugs targeting RTK signaling pathways ($n = 5$), i.e., RAS/ERK/MAPK and others (Fig. 6). On the other hand, it is resistant to drugs targeting six pathways, e.g., EGFR signaling, ERBB signaling and PI3K/Akt/mTOR signaling. It is worth noting that ABCB1 mRNA, which codes for multidrug resistance protein 1 (MDR1/P-gp), is highly and innately overexpressed in MLIA (Figure S4). This could be due to its enrichment in stem cells [49]. Concerning radiotherapy, MLIA appears to be one of the most radioresistant subtypes, as shown by high radiation sensitivity signature scores. As highlighted in the literature, chemo- and radioresistance may be related to cancer stem cell and mesenchymal features that define this subtype (Fig. 4; Table S6) [50]. Importantly, and despite immune activation, MLIA is above all characterized by dysfunctional CTL and a high TIDE score, meaning that ICB is probably less or not effective. However, this result needs to be confirmed. In this regard, there are not many ways to accurately estimate ICB response. Of the few available, the TIDE algorithm seems to perform well. In melanoma, mesenchymal phenotype, a hallmark of MLIA, is associated with innate anti-PD-1 resistance [51]. Additionally, the mesenchymal nature of this TNBC subtype could explain the prediction of low ICB response rates, together with chemo- and radioresistance. Overall, mesenchymal and stemness natures of MLIA reduce the chances of different treatment success.

The LAR subtype displays the most resistant profile to the panel of drugs screened (57 out of 198). Out of the different GOEA biological processes characterizing LAR, “response to xenobiotic stimulus” (GO:0009410) could explain this finding (Table S5). Indeed, eight out of the 10 selected genes involved in this pathway, highly expressed in LAR, were clearly linked to drug resistance in cancer (Table S7). These genes testify to the complex and multifactorial nature of drug-resistance mechanisms in LAR, such as increased drug metabolism (AKR genes, CYP genes), changes in drug efflux pumps (ABC genes) and elimination of cellular stress (AKR genes) [52]. In this study, the IC₅₀ was the highest in LAR subtype for doxorubicin, epirubicin, docetaxel, paclitaxel and tamoxifen, which are commonly used in BC treatment (Fig. 6; Table S7). On the other hand, this subtype seems to be particularly sensitive to drugs targeting the PI3K/Akt/mTOR signaling pathway ($n = 15$).

Availability of TNBC subtyping analysis on bc-GenExMiner

Transcriptomic data and their corresponding clinicopathological features of new TNBC cohorts were included in the bc-GenExMiner v5.0 database. TNBC molecular subtype assignment was done as described in the present study. As an example of practical application, four overexpressed genes between TNBC subtypes, identified by Burstein et al, were tested: DHRS2 for LAR, OGN for MLIA (MES), IDO1 for BLIA and ELF5 for BLIS [29]. The bc-GenExMiner v5.0 analyses confirmed the subtype specificity of these genes regardless of the nature of RNA measurement data (Figure S5).

Discussion

In this large cohort study, we identified four robust TNBC subtypes using unsupervised k-means consensus clustering analysis based on gene expression profiles: LAR, MLIA, BLIA and BLIS. We believe this molecular subtyping is robust for the following reasons: 1) it is based on a very large analysis, exploiting 1942 TNBC samples; 2) two types of transcriptomic data (i.e., microarrays [$n = 1243$] and RNAseq [$n = 699$]) were independently analyzed, 3) subtype annotation was assigned based on extensive gene enrichment analysis and 4) concordance with some previous research. Indeed, like ours, three studies clearly identified these four subtypes [29, 40, 53]. In addition, in Rody's study, although three TNBC subtypes were identified, it is worth noting that apocrine cluster is clearly divided into two subclusters, LAR and MLIA [30]. This supplementary subtype division is mainly based on immune response.

“Mesenchymal-like immune-altered” is a more accurate description of the fourth TNBC robust subtype, initially named mesenchymal stem-like and abbreviated as MSL/MES [17, 29]. In this way, the specific histological background, mesenchymal, and an important feature of the immune response, immune alteration, are highlighted.

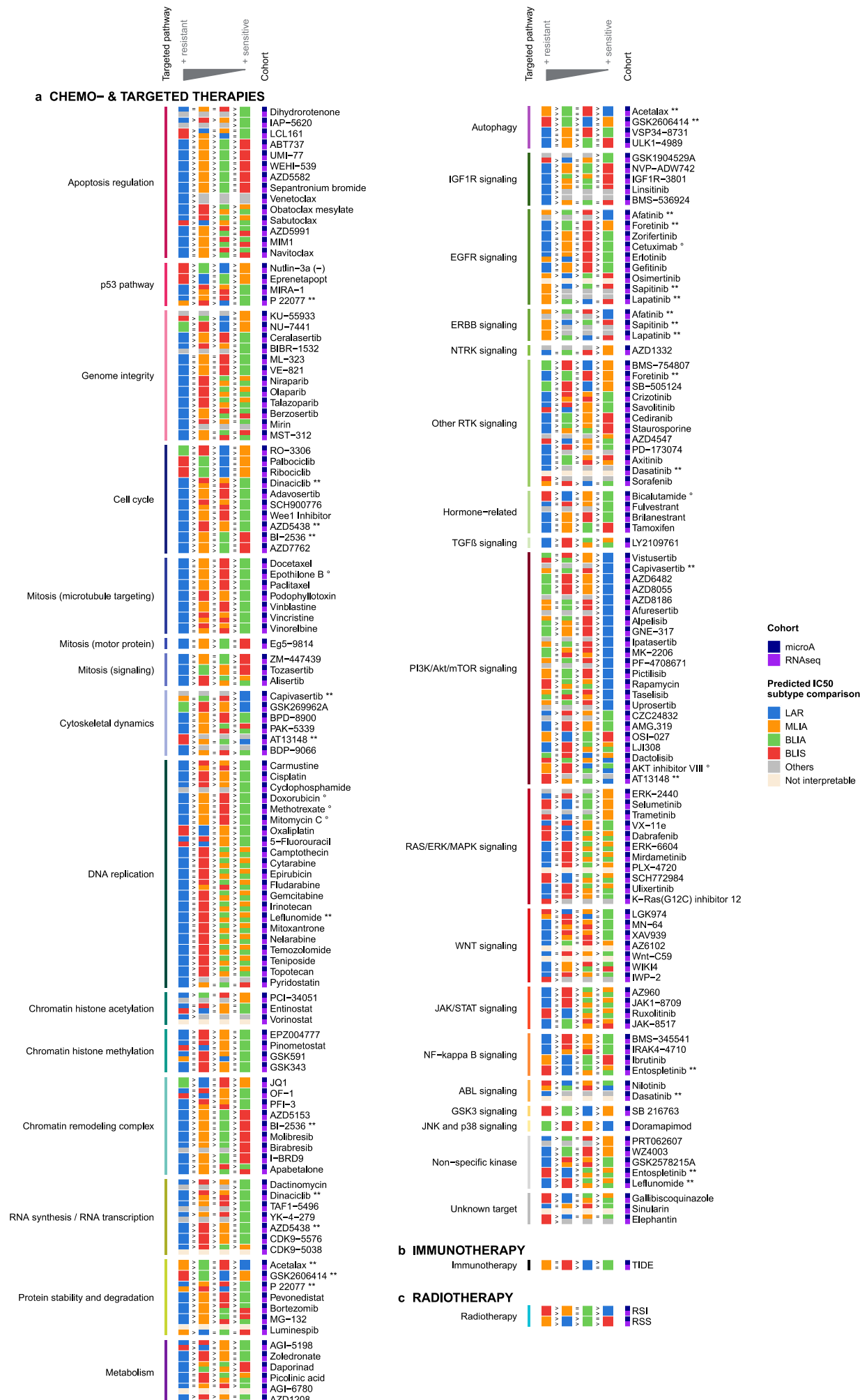


Figure 6: Prediction of treatment outcomes in TNBC subtypes. The four subtypes were compared according to treatment sensibility scores (detailed in a, b and c). Subtype pairwise comparison was performed using a Tukey post hoc test, where a P value threshold of 0.05 was used to define the equality or difference between subtype mean values. a Chemo- and targeted therapies response scores are predicted IC50, which were estimated using OncoPredict and pRRophetic packages. Treatments are classified according to their main biological target(s) (left row annotation). b Immune checkpoint blockade response was scored based on tumor immune dysfunction and exclusion (TIDE) algorithm. c Radiotherapy response scores were calculated using two gene expression signatures (see reference in Table S2) (**: various biological targets; °°: present in pRRophetic package).

At first glance, immune response spectra between MLIA and BLIA seem to be similar despite being found in different histological and biological backgrounds, notably marked EMT features in MLIA. Of note, mesenchymal trait is associated with tumor immune escape [47]. One important finding of the study, which needs validation, is the difference in terms of CTL functionality between MLIA and BLIA. Dysfunctional CTL state may result from the activation of the TGF β pathway, one of the main EMT drivers [36, 47]. In addition, CTL dysfunction in MLIA is associated with low ICB response prediction. Further studies are needed to explore if a causal link can be established between these two facts.

Robust TNBC molecular subtypes open up avenues for precision medicine because they are characterized by many drug targetable biological pathways. A wealth of articles have been written about this subject in recent years [7, 54, 55]. Here, we have focused on the MLIA subtype. As shown in our work, TNBC is a molecularly diverse disease, and its heterogeneity has likely limited the success of targeted therapies in unselected patients to date. Beside the recent approval of immune checkpoint inhibitors, chemotherapy and new generation of chemotherapy (i.e., antibody drug conjugated) remain the backbone of treatment. MLIA subtype harbors very distinct features, which could pave the way for dedicated treatment.

As previously discussed, despite high expression of immune checkpoint mRNAs, MLIA does not appear to be amenable to ICB as a first-line treatment. On the contrary, BLIA subtype is a promising candidate for such treatment.

A wide range of drugs targeting angiogenesis are being developed and approved for different tumor types. This pathway represents an important target for MLIA. Anti-angiogenic therapies have been developed in TNBC with mixed results. Bevacizumab has been widely tested in advanced and early TNBC and has been approved in the metastatic setting based on the E2100 study, showing a 5.5-month progression-free survival benefit [56]. However, given subsequent negative results, the Food and Drug Administration has withdrawn the approval contrary to the European Medicines Agency [57]. We hypothesize that selecting MLIA tumors could enhance the probability of demonstrating a clinical benefit compared to standard treatment.

EMT and MSL characteristics are particular features of MLIA compared to other subtypes. EMT is known to play an important role in cancer progression, metastasis, and resistance to chemotherapy and radiotherapy [47]. Preventing EMT by blocking the upstream extracellular signals and their signal transduction pathways is one of the strategies targeting EMT. In this context, the TGF β pathway represents an interesting target given its high activation in MLIA and the fact that it attenuates tumor response to PD-L1 inhibitors [58]. Several TGF β kinase inhibitors are in development. In a previous study, Galunisertib increased pathological complete response combined with neoadjuvant chemotherapy in rectal cancer, and hence could be tested in MLIA [59]. Binrafusp alfa is a bifunctional protein composed of the extracellular domain of the TGF β RII receptor (a TGF β "trap") fused to a humanized anti-PD-L1 IgG1 single-domain antibody. A phase II multicenter study of binrafusp alfa is ongoing as a monotherapy in HMGA2-expressing TNBC (NCT04489940). Here too, TGF β inhibition combined with immune checkpoint inhibitors could represent an interesting therapeutic strategy [60]. Additionally, the Wnt signaling pathway, involved in EMT is highly activated in MLIA. Several Wnt and β -catenin inhibitors are in development [61]. ST316 can selectively target the Wnt/ β -catenin signaling pathway and is currently evaluated in a phase I-II study with an expansion cohort in TNBC (NCT05848739). Finally, targeted regulation of epigenetics is a reversible and stable way of inducing the reprogramming required for phenotypic switching in the EMT process. Numerous epidrugs are currently in development and may be tested in MLIA.

STAT3, whose activation is linked to many cancer processes, could also represent an interesting target in MLIA tumors. Indeed, many STAT3 inhibitors have been developed and demonstrate anticancer activities both in vitro and in vivo TNBC models [62].

Today, through the identification of molecular heterogeneity of TNBC, it may be possible to understand part of the limited efficacy of therapies in unsubtyped TNBC patients. It is therefore of fundamental importance to subtype their tumors to improve their medical care. A recent and promising phase II clinical trial (FUTURE), which includes heavily pretreated metastatic TNBC, demonstrates that this approach is fruitful [63]. This pioneering study is encouraging because it demonstrates the validity and promise of a precision medicine approach for heavily pretreated metastatic TNBC.

Today there is no doubt that the era of precision medicine for TNBC patients has begun, and robust and consensual molecular subtyping of TNBC is a prerequisite for its success [64].

Supplementary information: The online version contains supplementary material available at https://static-content.springer.com/esm/art%3A10.1007%2Fs12282-024-01597-z/MediaObjects/12282_2024_1597_MOESM1_ESM.pdf

Acknowledgments: The research was supported by a grant from SIRIC ILIAD (INCa-DGOS-INSERM-ITMO Cancer_18011). We are most grateful to the Genomics and Bioinformatics Core Facility of Nantes (GenoBiRD, Biogenouest, IFB) for its technical support. The authors sincerely thank Alain Morel, Jonathan Dauvé and Sabrina Fronteau who carried out RNA-sequencing (GSE225002). We would also like to acknowledge Stacey Johnson for the English editing of the manuscript.

Author contributions: Conceptualization and design: PJ, HL and MC. Collection, assembly and curation of data: WG. Methodology and statistical analysis: PJ, HL, FBA, and BM. Data investigation and interpretation: PJ, HL, WG, JSF, MC and PPJ. Data visualization: AB, HL, PJ and WG. Writing-original draft preparation: PJ, HL, WG and JSF. Writing-review and editing: All authors. Final approval of manuscript: All authors.

Funding: GSE225002 RNA sequencing was supported by generous donations to the Institut de Cancérologie de l'Ouest for cancer research.

Data availability. Expression and patient clinical data of internal study were deposited in Gene Expression Omnibus (GEO) under the GSE225002 accession number. All cohorts/datasets used for the study are either publicly available or subject to written request to their owner. All codes used to analyze data can be obtained upon reasonable request from the corresponding author. No custom codes were developed.

Ethics approval and consent to participate. Regarding the GSE225002, the inclusion of the 48 patients was approved by the Ethics Committee of Angers University Hospital, France (ref #2023-192). Informed consent was obtained from patients to use their surgical specimens and clinicopathological data for research purposes, as required by the legal ethical authorities. All other data were publicly available.

Conflict of interest. The authors declare that they have no competing interests.

Références

- [1] Foulkes WD, Smith IE, Reis-Filho JS. Triple-negative breast cancer. *N Engl J Med* 2010;363:1938-48.
- [2] Liu Y, Hu Y, Xue J, Li J, Yi J, Bu J, et al. Advances in immunotherapy for triple-negative breast cancer. *Mol Cancer* 2023;22:145.
- [3] Patel SP, Kurzrock R. PD-L1 Expression as a Predictive Biomarker in Cancer Immunotherapy. *Mol Cancer Ther* 2015;14:847-56.
- [4] Schmid P, Cortes J, Pusztai L, McArthur H, Kümmel S, Bergh J, et al. Pembrolizumab for Early Triple-Negative Breast Cancer. *N Engl J Med* 2020;382:810-21.
- [5] Addala V, Newell F, Pearson JV, Redwood A, Robinson BW, Creaney J, et al. Computational immunogenomic approaches to predict response to cancer immunotherapies. *Nat Rev Clin Oncol* 2024;21:28-46.
- [6] Ahn SG, Kim SJ, Kim C, Jeong J. Molecular Classification of Triple-Negative Breast Cancer. *J Breast Cancer* 2016;19:223-30.
- [7] Garrido-Castro AC, Lin NU, Polyak K. Insights into Molecular Classifications of Triple-Negative Breast Cancer: Improving Patient Selection for Treatment. *Cancer Discov* 2019;9:176-98.
- [8] Ensenyat-Mendez M, Llinàs-Arias P, Orozco JJ, Íñiguez-Muñoz S, Salomon MP, Sesé B, et al. Current Triple-Negative Breast Cancer Subtypes: Dissecting the Most Aggressive Form of Breast Cancer. *Front Oncol* 2021;11:681476.
- [9] Sakach E, O'Regan R, Meisel J, Li X. Molecular Classification of Triple Negative Breast Cancer and the Emergence of Targeted Therapies. *Clin Breast Cancer* 2021;21:509-20.
- [10] Asleh K, Riaz N, Nielsen TO. Heterogeneity of triple negative breast cancer: Current advances in subtyping and treatment implications. *J Exp Clin Cancer Res* 2022;41:265.
- [11] Yu X, Liu Y, Chen M. Reassessment of Reliability and Reproducibility for Triple-Negative Breast Cancer Subtyping. *Cancers (Basel)* 2022;14:2571.

12. Stirzaker C, Zotenko E, Song JZ, Qu W, Nair SS, Locke WJ, et al. Methylome sequencing in triple-negative breast cancer reveals distinct methylation clusters with prognostic value. *Nat Commun* 2015;6:5899.
13. Masuda H, Qi Y, Liu S, Hayashi N, Kogawa T, Hortobagyi GN, et al. Reverse phase protein array identification of triple-negative breast cancer subtypes and comparison with mRNA molecular subtypes. *Oncotarget* 2017;8:70481-95.
14. Wang L, Lang GT, Xue MZ, Yang L, Chen L, Yao L, et al. Dissecting the heterogeneity of the alternative polyadenylation profiles in triple-negative breast cancers. *Theranostics* 2020;10:10531-47.
15. Asleh K, Negri GL, Spencer Miko SE, Colborne S, Hughes CS, Wang XQ, et al. Proteomic analysis of archival breast cancer clinical specimens identifies biological subtypes with distinct survival outcomes. *Nat Commun* 2022;13:896.
16. Gong TQ, Jiang YZ, Shao C, Peng WT, Liu MW, Li DQ, et al. Proteome-centric cross-omics characterization and integrated network analyses of triple-negative breast cancer. *Cell Rep* 2022;38:110460.
17. Lehmann BD, Bauer JA, Chen X, Sanders ME, Chakravarthy AB, Shyr Y, et al. Identification of human triple-negative breast cancer subtypes and preclinical models for selection of targeted therapies. *J Clin Invest* 2011;121:2750-67.
18. Lehmann BD, Jovanović B, Chen X, Estrada MV, Johnson KN, Shyr Y, et al. Refinement of Triple-Negative Breast Cancer Molecular Subtypes: Implications for Neoadjuvant Chemotherapy Selection. *PLoS One* 2016;11:e0157368.
19. Chiu AM, Mitra M, Boymoushakian L, Coller HA. Integrative analysis of the inter-tumoral heterogeneity of triple-negative breast cancer. *Sci Rep* 2018;8:11807.
20. Jézéquel P, Kerdraon O, Hondermarck H, Guérin-Charbonnel C, Lasla H, Gouraud W, et al. Identification of three subtypes of triple-negative breast cancer with potential therapeutic implications. *Breast Cancer Res* 2019;21:65.
21. Prado-Vázquez G, Gámez-Pozo A, Trilla-Fuertes L, Arevalillo JM, Zapater-Moros A, Ferrer-Gómez M, et al. A novel approach to triple-negative breast cancer molecular classification reveals a luminal immune-positive subgroup with good prognoses. *Sci Rep* 2019;9:1538.
22. Bareche Y, Venet D, Ignatiadis M, Aftimos P, Piccart M, Rothe F, et al. Unravelling triple-negative breast cancer molecular heterogeneity using an integrative multiomic analysis. *Ann Oncol* 2018;29:895-902.
23. Emens LA. Breast Cancer Immunotherapy: Facts and Hopes. *Clin Cancer Res* 2018;24:511-20.
24. Abdou Y, Goudarzi A, Yu JX, Upadhyaya S, Vincent B, Carey LA. Immunotherapy in triple negative breast cancer: beyond checkpoint inhibitors. *NPJ Breast Cancer* 2022;8:121.
25. Brown LC, Loi S. Immune checkpoint inhibition in the treatment of early stage triple negative breast cancer: 2021 update. *Breast* 2022;62 Suppl 1:S29-S33.
26. Howard FM, Pearson AT, Nanda R. Clinical trials of immunotherapy in triple-negative breast cancer. *Breast Cancer Res Treat* 2022;195:1-15.
27. Lehmann BD, Colaprico A, Silva TC, Chen J, An H, Ban Y, et al. Multi-omics analysis identifies therapeutic vulnerabilities in triple-negative breast cancer subtypes. *Nat Commun* 2021;12:6276.
28. Bareche Y, Buisseret L, Grusso T, Girard E, Venet D, Dupont F, et al. Unraveling Triple-Negative Breast Cancer Tumor Microenvironment Heterogeneity: Towards an Optimized Treatment Approach. *J Natl Cancer Inst* 2020;112:708-19.
29. Burstein MD, Tsimelzon A, Poage GM, Covington KR, Contreras A, Fuqua SA, et al. Comprehensive genomic analysis identifies novel subtypes and targets of triple-negative breast cancer. *Clin Cancer Res* 2015;21:1688-98.
30. Rody A, Karn T, Liedtke C, Puszta L, Ruckhaeberle E, Hanker L, et al. A clinically relevant gene signature in triple negative and basal-like breast cancer. *Breast Cancer Res* 2011;13:R97.
31. Jézéquel P, Campone M, Gouraud W, Guérin-Charbonnel C, Leux C, Ricolleau G, et al. bc-GenExMiner: an easy-to-use online platform for gene prognostic analyses in breast cancer. *Breast Cancer Res Treas*. 2012;131:765-75.
32. Jézéquel P, Frénel JS, Campion L, Guérin-Charbonnel C, Gouraud W, Ricolleau G, et al. bc-GenExMiner 3.0: new mining module computes breast cancer gene expression correlation analyses. *Database (Oxford)* 2013;2013:bas060.
33. Jézéquel P, Gouraud W, Ben Azzouz F, Guérin-Charbonnel C, Juin PP, Lasla H, et al. bc-GenExMiner 4.5: new mining module computes breast cancer differential gene expression analyses. *Database (Oxford)* 2021;2021:baab007.
34. Maeser D, Gruener RF, Huang RS. oncoPredict: an R package for predicting in vivo or cancer patient drug response and biomarkers from cell line screening data. *Brief Bioinform* 2021;22:bbab260.
35. Wherry EJ, Kurachi M. Molecular and cellular insights into T cell exhaustion. *Nat Rev Immunol* 2015;15:486-99.
36. Massagué J. TGFbeta in Cancer. *Cell* 2008;134:215-30.
37. Torti SV, Torti FM. Iron and cancer: more ore to be mined. *Nat Rev Cancer* 2013;13:342-55.
38. DeBerardinis RJ, Chandel NS. Fundamentals of cancer metabolism. *Sci Adv* 2016;2:e1600200.
39. Shin E, Koo JS. Glucose Metabolism and Glucose Transporters in Breast Cancer. *Front Cell Dev Biol* 2021;9:728759.
40. Jiang YZ, Ma D, Suo C, Shi J, Xue M, Hu X, et al. Genomic and Transcriptomic Landscape of Triple-Negative Breast Cancers: Subtypes and Treatment Strategies. *Cancer Cell* 2019;35:428-40.
41. Herschkowitz JI, Simin K, Weigman VJ, Mikaelian I, Usary J, Hu Z, et al. Identification of conserved gene expression features between murine mammary carcinoma models and human breast tumors. *Genome Biol* 2007;8:R76.
42. Creighton CJ, Li X, Landis M, Dixon JM, Neumeister VM, Sjolund A, et al. Residual breast cancers after conventional therapy display mesenchymal as well as tumor-initiating features. *Proc Natl Acad Sci U S A* 2009;106:13820-5.
43. Prat A, Parker JS, Karginova O, Fan C, Livasy C, Herschkowitz JI, et al. Phenotypic and molecular characterization of the claudin-low intrinsic subtype of breast cancer. *Breast Cancer Res* 2010;12:R68.
44. Ginestier C, Hur MH, Charafe-Jauffret E, Monville F, Dutcher J, Brown M, et al. ALDH1 is a marker of normal and malignant human mammary stem cells and a predictor of poor clinical outcome. *Cell Stem Cell* 2007;1:555-67.

45. Xu J, Lamouille S, Deryck R. TGF-beta-induced epithelial to mesenchymal transition. *Cell Res* 2009;19:156-72.
46. Nieto MA, Huang RY, Jackson RA, Thiery JP. EMT: 2016. *Cell* 2016;166:21-45.
47. Terry S, Savagner P, Ortiz-Cuaron S, Mahjoubi L, Saintigny P, Thiery JP, et al. New insights into the role of EMT in tumor immune escape. *Mol Oncol* 2017;11:824-46.
48. Joyce JA, Fearon DT. T cell exclusion, immune privilege, and the tumor microenvironment. *Science* 2015;348:74-80.
49. Holohan C, Van Schaeybroeck S, Longley DB, Johnston PG. Cancer drug resistance: an evolving paradigm. *Nat Rev Cancer* 2013;13:714-26.
50. Baumann M, Krause M, Hill R. Exploring the role of cancer stem cells in radioresistance. *Nat Rev Cancer* 2008;8:545-54.
51. Hugo W, Zaretsky JM, Sun L, Song C, Moreno BH, Hu-Lieskovay S, et al. Genomic and Transcriptomic Features of Response to Anti-PD-1 Therapy in Metastatic Melanoma. *Cell* 2017;168:542.
52. Penning TM, Jonnalagadda S, Trippier PC, Rižner TL. Aldo-Keto Reductases and Cancer Drug Resistance. *Pharmacol Rev* 2021;73:1150-71.
53. Liu YR, Jiang YZ, Xu XE, Yu KD, Jin X, Hu X, et al. Comprehensive transcriptome analysis identifies novel molecular subtypes and subtype-specific RNAs of triple-negative breast cancer. *Breast Cancer Res* 2016;18:33.
54. Bianchini G, Balko JM, Mayer IA, Sanders ME, Gianni L. Triple-negative breast cancer: challenges and opportunities of a heterogeneous disease. *Nat Rev Clin Oncol* 2016;13:674-90.
55. Keenan TE, Tolane SM. Role of Immunotherapy in Triple-Negative Breast Cancer. *J Natl Compr Canc Netw* 202;18:479-89.
56. Miller K, Wang M, Gralow J, Dickler M, Cobleigh M, Perez EA, et al. Paclitaxel plus bevacizumab versus paclitaxel alone for metastatic breast cancer. *N Engl J Med* 2007;357:2666-76.
57. Sasich LD, Sukkari SR. The US FDAs withdrawal of the breast cancer indication for Avastin (bevacizumab). *Saudi Pharm J* 2012;20:381-5.
58. Mariathasan S, Turley SJ, Nickles D, Castiglioni A, Yuen K, Wang Y, et al. TGF β attenuates tumour response to PD-L1 blockade by contributing to exclusion of T cells. *Nature* 2018;554:544-8.
59. Yamazaki T, Gunderson AJ, Gilchrist M, Whiteford M, Kiely MX, Hayman A, et al. Galunisertib plus neoadjuvant chemoradiotherapy in patients with locally advanced rectal cancer: a single-arm, phase 2 trial. *Lancet Oncol* 2022;23:1189-200.
60. Metropulos AE, Munshi HG, Principe DR. The difficulty in translating the preclinical success of combined TGF β and immune checkpoint inhibition to clinical trial. *EBioMedicine* 2022;86:104380.
61. Jung YS, Park JI. Wnt signaling in cancer: therapeutic targeting of Wnt signaling beyond β -catenin and the destruction complex. *Exp Mol Med* 2020;52:183-91.
62. Qin JJ, Yan L, Zhang J, Zhang WD. STAT3 as a potential therapeutic target in triple negative breast cancer: a systematic review. *J Exp Clin Cancer Res* 2019;38:195.
63. Liu Y, Zhu XZ, Xiao Y, Wu SY, Zuo WJ, Yu Q, et al. Subtyping-based platform guides precision medicine for heavily pretreated metastatic triple-negative breast cancer: The FUTURE phase II umbrella clinical trial. *Cell Res* 2023;33:389-402.
64. Pascual J, Turner NC. Targeting the PI3-kinase pathway in triple-negative breast cancer. *Ann Oncol* 2019;30:1051-60.